Iterative Analysis of Exchange-Broadened NMR Band Shapes. The Mechanism of Correlated Rotations in Triaryl Derivatives of Phosphorus and Arsenic

Eva E. Wille, David S. Stephenson, Peter Capriel, and Gerhard Binsch*

Contribution from the Institute of Organic Chemistry, University of Munich, D-8000 Munich 2, West Germany. *Received September 15, 1980*

Abstract: Tris[2,6-bis(difluoromethyl)phenyl]phosphine and tris[2,6-bis(difluoromethyl)phenyl]arsine as well as the corresponding oxides have been synthesized. The ^{19}F NMR data extracted from the static spectra at low temperature rigorously establish that all four compounds adopt a chiral propeller equilibrium conformation in solution. A theoretical analysis of the conformational dynamics allows for seven differentiable permutational mechanisms (M_1–M_7), of which five (M_1–M_4, M_7) could be experimentally excluded on the basis of the fast-exchange limit spectra. Iterative band shape analyses of the exchange-broadened spectra for the remaining two possibilities (M_5, M_6) and for two alternative relative assignments of the ^{19}F chemical shifts simultaneously yielded the correct assignment as well as direct and quantitative proof for the exclusive operation of the permutational mechanism M_5, which corresponds to a process commonly referred to in the literature as the "two-ring flip". The relative shift assignment was independently confirmed by a selective population inversion experiment on the arsenic compound. The skeleton of a density matrix theory for the latter experiment is outlined in the Appendix.

The dynamic analysis of exchange-broadened NMR band shapes has been routinely possible for many years.[1] Prior to 1978, however, one had to rely on a synthetic approach for all but the simplest spin systems. This procedure, in which theoretical trial spectra, computed from guessed parameter values, are visually compared with the experimental band shapes, is in general perfectly adequate as long as the exchange scheme is sufficiently simple and the assignments can easily be deduced from the spectra, but ceases to be so in more complicated cases, especially for multiple rate processes.[2] We have recently described[3] an efficient and stable iterative technique which operates directly on the raw digitized band shapes as they are produced by a modern NMR spectrometer and which yields the optimum parameters automatically, together with an error analysis. In the present paper we report on a specific application to a situation where such an automated method proved indispensable even for qualitative purposes.

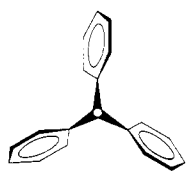

1

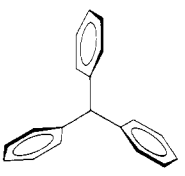

2

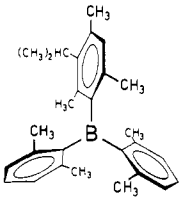

3

We shall be concerned with triaryl compounds of the general formula Ar_3ZL, where L is a ligand of effective rotational symmetry or a free electron pair and where in the latter case the central atom Z is assumed to retain its pyramidal configuration on the NMR time scale.[4] Two questions, one of structure and one of dynamics, arise in this context. An X-ray analysis of trimesitylmethane[5a] and trimesitylphosphine[5b] established the basic chiral propeller structure **1** of C_3 symmetry in the crystal. It is therefore likely that **1** is in general the preferred conformation also in solution, but it would of course be desirable to obtain direct experimental proof for this extrapolation. A restricted internal rotation in trimesityl derivatives of phosphorus and arsenic had been detected by Rieker and Kessler[6] as early as 1969. The mechanism of this process has subsequently been investigated in great detail,[7,8] especially by Mislow and co-workers.[7,8a-j] Provided that **1** is indeed the equilibrium structure in solution, it is easily seen that there are in fact seven differentiable possibilities. In the first (M_1), one of the phenyl rings undergoes a rotation by 180° at a time. Following Mislow,[7b] we call this an edge interchange, symbolized by e. It is obviously a threefold degenerate process and leaves the helicity of the molecule unaffected. Edge interchanges can be performed on two rings simultaneously (e^2, M_2) or on all three rings (e^3, M_3), the latter being a nondegenerate process. Then there can be the nondegenerate act of helicity reversal (h, M_4) which involves a motion of all three rings such that all ortho substituents maintain their proximal or distal relationships to the ligand L; a reasonable chemical transition state for it is shown schematically in Figure 1. The final three possibilities M_5–M_7 of Figure 1 are obtained by a combination of h with the distinct edge interchanges. Clearly, this list exhausts the differentiable possibilities of correlated motions in Ar_3ZL that do not involve the breaking of bonds or atomic inversion, as can also be shown by formal reasoning[7] based on group- or graph-theoretical principles.

Systematic empirical force field calculations[8e,i,j] and NMR studies on a variety of unsymmetrically substituted derivatives[8f,h,k] have already furnished strong theoretical and indirect experimental evidence for an equilibrium propeller conformation in solution and for the preferred operation of the so-called[7] two-ring flip mechanism, which corresponds to M_5 (Figure 1) in our notation. Perhaps the most convincing piece of experimental support comes from a DNMR study of the boron derivative **3**.[9] Although this compound belongs to the general class Ar_3Z with a trigonal central atom Z, whose parent presumably has the D_3 symmetry of **2** and

(1) For a recent review, see: Binsch, G.; Kessler, H. *Angew. Chem., Int. Ed. Engl.* **1980**, *19*, 411–428.
(2) Höfner, D.; Stephenson, D. S.; Binsch, G. *J. Magn. Reson.* **1978**, *32*, 131–144.
(3) Stephenson, D. S.; Binsch, G. *J. Magn. Reson.* **1978**, *32*, 145–152.
(4) This condition is well known to be satisfied for phosphorus and arsenic as the central atom Z: (a) Kessler, H. *Angew. Chem., Int. Ed. Engl.* **1970**, *9*, 219–235. (b) Rauk, A.; Allen, L. C.; Mislow, K. *Ibid.* **1970**, *9*, 400–415. (c) Lambert, J. B. *Top. Stereochem.* **1971**, *6*, 19–105.
(5) (a) Blount, J. F.; Mislow, K. *Tetrahedron Lett.* **1975**, 909–912. (b) Blount, J. F.; Maryanoff, C. A.; Mislow, K. *Ibid.* **1975**, 913–916.
(6) Rieker, A.; Kessler, H. *Tetrahedron Lett.* **1969**, 1227–1230.
(7) For reviews, see: (a) Mislow, K.; Gust, D.; Finocchiaro, P.; Boettcher, R. J. *Top. Curr. Chem.* **1974**, *47*, 1–28. (b) Mislow, K. *Acc. Chem. Res.* **1976**, *9*, 26–33.
(8) (a) Gust, D.; Mislow, K. *J. Am. Chem. Soc.* **1973**, *95*, 1535–1547. (b) Boettcher, R. J.; Gust, D., Mislow, K. *Ibid.* **1973**, *95*, 7157–7158. (c) Finocchiaro, P.; Gust, D.; Mislow, K. *Ibid.* **1973**, *95*, 8172–8173. (d) Finocchiaro, P.; Gust, D.; Mislow, K. *Ibid.* **1974**, *96*, 2165–2167. (e) Andose, J. D.; Mislow, K. *Ibid.* **1974**, *96*, 2168–2176. (f) Finocchiaro, P.; Gust, D.; Mislow, K. *Ibid.* **1974**, *96*, 2176–2182. (g) Finocchiaro, P.; Gust, D.; Mislow, K. *Ibid.* **1974**, *96*, 3198–3205. (h) Finocchiaro, P.; Gust, D.; Mislow, K. *Ibid.* **1974**, *96*, 3205–3213. (i) Kates, M. R.; Andose, J. D.; Finocchiaro, P.; Gust, D.; Mislow, K. *Ibid.* **1975**, *97*, 1772–1778. (j) Hummel, J. P.; Zurbach, E. P.; DiCarlo, E. N.; Mislow, K. *Ibid.* **1976**, *98*, 7480–7483. (k) Willem, R.; Hoogzand, C. *Org. Magn. Reson.* **1979**, *12*, 55–58.
(9) Hummel, J. P.; Gust, D.; Mislow, K. *J. Am. Chem. Soc.* **1974**, *96*, 3679–3681.

0002-7863/82/1504-0405$01.25/0

Table I. ^{19}F Chemical Shifts (Hz)[a] for the [[ABXCDY]$_3$M] Spin Systems of 4–7 in Acetone-d_6

compd	temp, °C	ν_A	ν_B	ν_C	ν_D
4	−80.4	−11 223.62 (2)	−9 427.17 (2)	−10 117.75 (2)	−10 501.60 (2)
5	−91.7	−11 141.15 (3)	−9 464.23 (3)	−10 057.49 (3)	−10 385.76 (3)
6	−2.7	−10 593.17 (2)	−9.846.24 (3)	−9 808.51 (3)	−10 173.83 (3)
7	−23.3	−11 085.66 (1)	−9 644.16 (3)	−9 795.91 (2)	−10 240.24 (3)

[a] At 94.08 MHz relative to external 15:85 $CFCl_3$–acetone-d_6.

Table II. Geminal Coupling Constants (Hz) for the [[ABXCDY]$_3$M] Spin Systems of 4–7 in Acetone-d_6

compd	temp, °C	$\lvert J_{AB}\rvert$	$\lvert J_{CD}\rvert$	$\lvert J_{AX}\rvert$	$\lvert J_{BX}\rvert$	$\lvert J_{CY}\rvert$	$\lvert J_{DY}\rvert$
4	−80.4	295.73 (3)	302.73 (6)	53.22 (4)	54.66 (4)	54.26 (4)	54.21 (4)
5	−91.7	294.87 (4)	301.42 (8)	52.92 (5)	54.99 (5)	54.15 (5)	54.00 (5)
6	−2.7	301.43 (4)	307.58 (7)	54.16 (3)	54.49 (5)	54.26 (5)	53.80 (5)
7	−23.3	298.02 (2)	307.14 (6)	55.33 (3)	54.64 (8)	53.86 (7)	53.69 (8)

is therefore not strictly relevant to the Ar_3ZL type under consideration here, the analogy is close enough to be at least suggestive. It does not appear to have been recognized, however, that there exists the prospect of adducing direct experimental proof for the conclusions from the investigation of judiciously designed model compounds Ar_3ZL containing three identical, symmetrically substituted phenyl rings.

The possibility of such a proof hinges on the introduction of prochiral CU_2V substituents into all ortho (and/or meta) positions. If the molecule indeed assumes the preferred propeller conformation **1** in solution, the two ortho substituents of a phenyl ring are rendered diastereotopic as are the U groups of each substituent, thus giving rise to U nuclei in four distinct environments. These U groups can then serve the double purpose of sensing the elementary dynamic process of edge interchange e as well as the act of helicity reversal h. As will be shown in more detail below, the 12 U nuclei are in principle sufficient for differentiating between all seven permutational mechanisms. In order to have a realistic chance of succeeding in this endeavor also in practice, one requires an NMR sensor nucleus which has a magnetic moment large enough to permit a quantitative band shape analysis over the entire range of exchange broadening and whose chemical shift responds in a very sensitive fashion to nonbonded interactions. It is clear that only the ^{19}F spin satisfies both of these prerequisites.[10]

Results and Discussion

Syntheses. In view of the logical and practical constraints to be imposed, the chemical structure of suitable target molecules is largely predetermined, except for the nature of Z and L. The synthetic scheme employed in the preparation of the four model compounds **4–7** is shown in Chart I. The synthesis of the common precursor 2,6-bis(difluoromethyl)bromobenzene involves only standard procedures, but the conversion to **4** and **5** is critical not only because the reaction is sterically rather demanding but also because of the uncertainty concerning the survival of the difluoromethyl substituents under the necessarily strongly basic reaction conditions. It therefore came as no surprise that the latter step resulted in a mixture consisting of numerous components, from which the desired compounds could be isolated only in poor yields, especially in the case of **4** (2%). The conversion to the corresponding oxides **6** and **7**, on the other hand, presented no difficulties.

All four compounds **4–7** could be obtained as pure crystalline solids, but whereas **6** and **7** are also stable in solution, **4** and **5** suffer gradual decompositions in acetone-d_6 at room temperature. In the case of **5** this process is slow enough so as not to affect the spectroscopic studies adversely, but is more serious for **4**, with consequences to be discussed later. The peculiar observations suggest that the decomposition mode may have to be attributed to a bimolecular attack of the nucleophilic Z atom on one of the difluoromethyl groups, but no effort was made to determine the nature of the relevant processes rigorously.

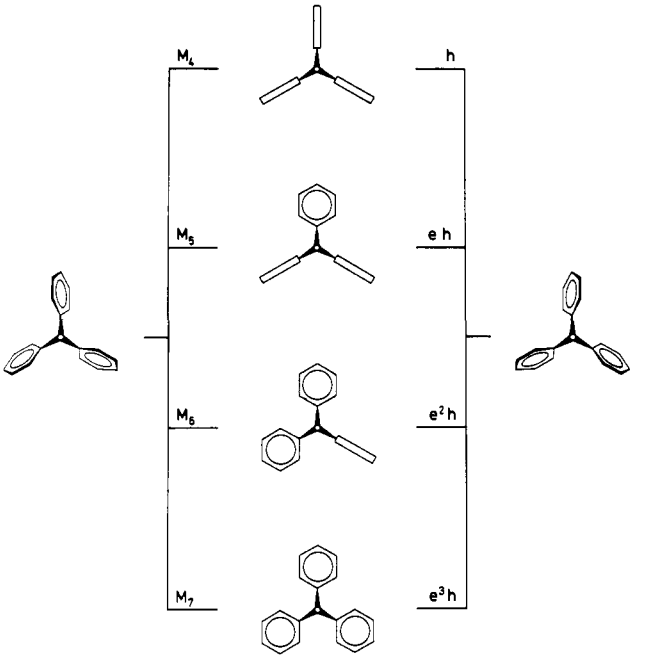

Figure 1. Idealized chemical transition states for the permutational mechanisms M_4–M_7.

Chart I

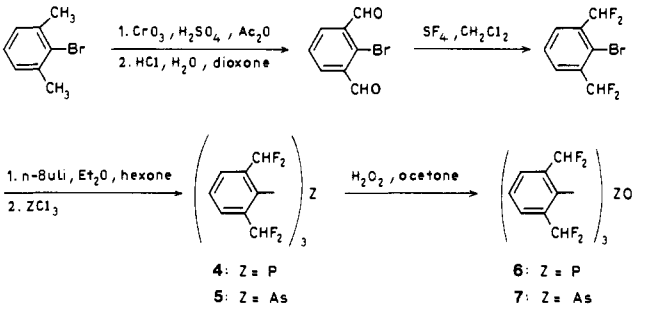

Static NMR Spectra and Permutational Schemes. A structure of C_3 symmetry necessitates that the slow-exchange limit NMR spectra of **4–7** be those of an [[ABXCDY]$_3$M] spin system,[11] where the labels ABCD and XY refer to the ^{19}F and ^1H spins of the difluoromethyl substituents, respectively, and M to ^{31}P or ^{75}As, the latter having a spin quantum number of $^3/_2$. This is in fact precisely what one observes in all four cases, thus at once providing the rigorous proof of the propeller equilibrium conformation *in solution*. The ^{19}F NMR spectrum of **5** at −91.7 °C is particularly

(10) The unique suitability of the difluoromethyl group for mechanistic DNMR studies has been exploited in a similar context: Rakshys, J. W.; McKinley, S. V.; Freedman, H. H. *J. Am. Chem. Soc.* **1971**, *93*, 6522–6529.

(11) The notation employed throughout this paper is that of Haigh: Haigh, C. W. *J. Chem. Soc. A* **1970**, 1682–1683.

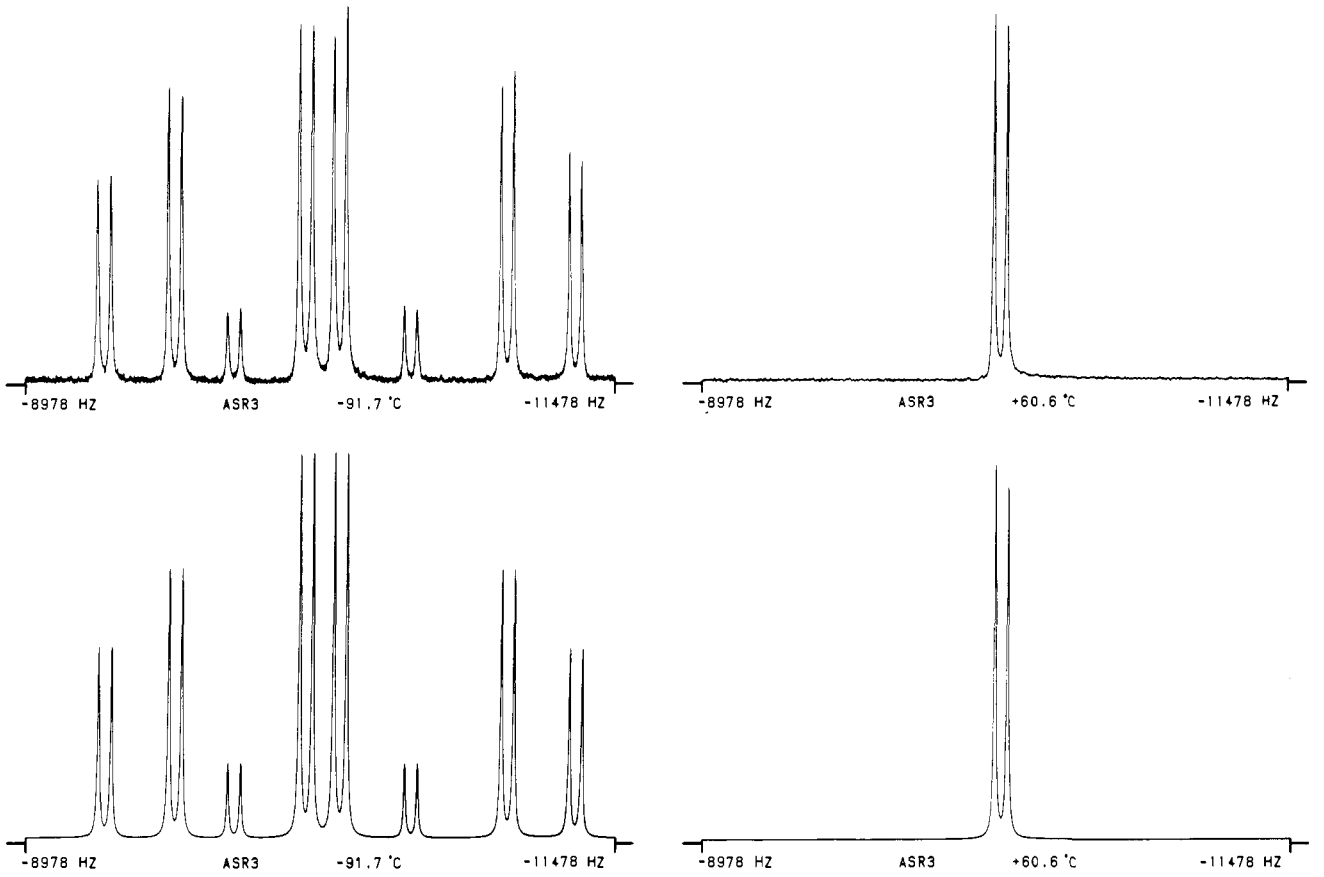

Figure 2. Observed and computed 94.08 MHz ^{19}F NMR spectra of **5** in acetone-d_6 at −91.7 °C (left) and +60.6 °C (right).

Table III. Resolved Long-Range Coupling Constants (Hz) for the [[ABXCDY]$_3$M] Spin Systems of **4**, **6**, and **7** in Acetone-d_6

compd	temp, °C	$\|J_{AM}\|$	$\|J_{BM}\|$	$\|J_{CM}\|$	$\|J_{DM}\|$	$\|J_{\langle XY\rangle M}\|^a$
4	−80.4	18.46 (4)	21.33 (4)	3.09 (4)	2.83 (4)	3.2
6	−2.7	*b*	5.65 (5)	4.91 (5)	5.50 (5)	b
7	−23.3	*b*	2.52 (2)	3.31 (2)	2.79 (2)	b

[a] Averaged value extracted from the ^1H NMR spectrum at ambient temperature. [b] Not resolved.

Table IV. ^{19}F NMR Characteristics of the Permutational Mechanisms

mechanism	type	degeneracy	elementary exchange act	fast exchange limit	
				complete	truncated
M_1	e	3	[CDAB][ABCD]$_2$	[[⟨AC⟩⟨BD⟩]$_2$]$_3$	1 ⟨AC⟩⟨BD⟩ type
M_2	e^2	3	[CDAB]$_2$[ABCD]	[[⟨AC⟩⟨BD⟩]$_2$]$_3$	1 ⟨AC⟩⟨BD⟩ type
M_3	e^3	1	[CDAB]$_3$	[⟨AC⟩⟨BD⟩]$_6$	1 ⟨AC⟩⟨BD⟩ type
M_4	h	1	[BADC]$_3$	[⟨AB⟩⟨CD⟩]$_6$	2 singlets
M_5	he	3	[DCBA][BADC]$_2$	[⟨ABCD⟩$_{12}$]	1 singlet
M_6	he^2	3	[DCBA]$_2$[BADC]	[⟨ABCD⟩$_{12}$]	1 singlet
M_7	he^3	1	[DCBA]$_3$	[⟨AD⟩⟨BC⟩]$_6$	1 ⟨AD⟩⟨BC⟩ type

clean-cut (Figure 2) owing to the circumstance that in this case all long-range coupling constants happen to fall below the detection limit set by the line width. The low-temperature static NMR spectra of **4**, **6**, and **7** are richer in lines, but their automated analysis, using the computer program DAVINS,[12] was just as straightforward. These analyses were repeated at a series of temperatures below the onset of exchange broadening in order to obtain information on the temperature dependence of the static parameters. The results for one particular temperature in each case are listed in Tables I–III.

In analyzing the consequences of the permutational mechanisms (each one taken individually, henceforth denoted as "pure") for the appearance of the NMR spectra, the nuclei X, Y, and M are largely irrelevant, since they do not furnish mechanistic information beyond that already present in the fluorine spin system and may hence be omitted from consideration; in other words, it suffices to focus the attention on the dynamic fate of an [ABCD]$_3$ system.[13] The result of an elementary exchange act on this reference configuration is displayed in column 4 of Table IV and the spin system of the fast-exchange limit spectrum in column 5. In describing the latter we employ an extension of the standard notation[11] by using angular as well as square brackets. The contents of an angular bracket denote a *single* spin in an averaged environment and the enclosed nuclear labels indicate the nature of the averaging process.

As can be gleaned from Table IV, a partial distinction between the seven pure mechanisms is *in principle* already possible on the basis of the static fast-exchange limit spectra, for which one

(12) Stephenson, D. S.; Binsch, G. *J. Magn. Reson.* **1980**, *37*, 395–407, 409–430; *QCPE* **1979**, *11*, 378.

(13) In the dynamic calculations, to be discussed in the next subsection, suitable account must of course be taken of the additional first-order splittings.

ABX	$\frac{2}{3}k_5 + \frac{1}{3}k_6$	0	$\frac{1}{3}k_5 + \frac{2}{3}k_6$
$\frac{2}{3}k_5 + \frac{1}{3}k_6$	BAX	$\frac{1}{3}k_5 + \frac{2}{3}k_6$	0
0	$\frac{1}{3}k_5 + \frac{2}{3}k_6$	CDY	$\frac{2}{3}k_5 + \frac{1}{3}k_6$
$\frac{1}{3}k_5 + \frac{2}{3}k_6$	0	$\frac{2}{3}k_5 + \frac{1}{3}k_6$	DCY

Figure 3. A schematic representation indicating the off-diagonal blocks of the exchange matrices in composite spin Liouville space.

predicts five different types.[14] Whether these distinctions can *all* be made *in practice* depends of course on the detectability of the relevant discriminating features in the spectra. Since the isotropic $^6J_{FF}$ and $^8J_{FF}$ coupling constants were invariably found to be too small to be resolved in **4–7**, this condition is not satisfied completely. In fact, setting these unobserved long-range J_{FF} couplings to zero rigorously, one obtains the truncated spectral types listed in the last column of Table IV. In this truncated set a static distinction between $\{M_1, M_2\}$ and M_3 is no longer feasible in isotropic solution; to recover it one would have to investigate the compounds in liquid crystal solvents, although admittedly the spectra would then be expected to exhibit such a high degree of complexity as to severely tax even the most advanced methods[15] of analysis. As it turns out, however, these imagined difficulties are academic, since the fast-exchange limit ^{19}F NMR spectra of **4–7** are experimentally found to be all of the $[\langle ABCD\rangle_{12}]$ type, apart from heteronuclear splittings, and thus immediately allow one to narrow down the pure mechanistic possibilities to just M_5 and M_6. The phenomenologically simplest case is again that of **5**, from which all heteronuclear long-range couplings are absent; the static ^{19}F NMR spectrum at 60.6 °C consists of just two lines separated by $J_{\langle ABCD\rangle\langle XY\rangle}$, as shown in Figure 2.

In concluding this subsection we remark that the static ^1H NMR spectra furnish a fully consistent picture, as of course they must in view of the fact that the conclusions already arrived at follow from the observations via a logically impeccable chain of arguments. At low temperature one observes basically two triplets for the methine protons of the difluoromethyl substituents, which in **4** exhibit additional doublet fine structure arising from coupling to ^{31}P, whereas long-range couplings in **5–7** only manifest themselves through differential line broadenings. The corresponding high-temperature patterns are a single triplet for **5–7** and a triplet of doublets for **4**. Since these spectra only contain a trivial fraction of the mechanistic information, it was not considered worthwhile to subject them to quantitative static and dynamic analysis. With the exception of a single number cited in Table III, the approximate NMR parameters extracted from the ^1H NMR spectra are relegated to the Experimental Section.

(14) For the edification of readers interested in formal aspects, who may be wondering about the difference between an $[\langle AC\rangle\langle BD\rangle]_6$ and an $[[\langle AC\rangle\langle BD\rangle_2]_3$ spin system, we mention that of the $(12!/2!10!)/3 = 22$ distinct coupling constants in $[ABCD]_3$ there remain 12 in $[\langle AC\rangle\langle BD\rangle]_6$ but only 8 in $[[\langle AC\rangle\langle BD\rangle]_2]_3$ that can in principle be extracted from the spectra. Another way of rendering the nomenclature more specific would be to append group-theoretical symbols indicating the isomorphism of the pertinent effective nuclear permutation groups to symmetry point groups. We have refrained from cluttering up the notation in Table IV unnecessarily, however, since column 5 as it reads already shows that theory predicts five distinct fast-exchange limit spectra for the seven permutational mechanisms, and that is all that is of concern to us at this juncture.

(15) Stephenson, D. S.; Binsch, G. *Org. Magn. Reson.* **1980**, *14*, 226–233; *Mol. Phys.* **1981**, *43*, 697–710.

Table V. Some Iteratively Calculated Rate Constants for the Processes M_5 and M_6 of **5** and Their Standard Deviations

temp, °C	assignment 1		assignment 2	
	k_5, s^{-1}	k_6, s^{-1}	k_5, s^{-1}	k_6, s^{-1}
−46.8	405.0 (10.5)	2.1 (8.9)	415.8 (5.6)	0.9 (4.7)
−41.1	546.4 (15.8)	58.6 (15.3)	654.6 (5.9)	0.7 (4.3)
−38.6	727.0 (20.4)	16.1 (16.9)	805.3 (8.0)	0.8 (5.2)
−31.4	569.0 (34.9)	543.6 (32.8)	1366.0 (12.6)	0.6 (6.5)

Band Shape Studies. Having approached the truth by means of Holmes' principle,[16] the final distinction between pure M_5 and M_6 has to be sought in the exchange-broadened band shapes which, as evident from column 4 of Table IV, must indeed contain the discriminating characteristic in principle.[17] A convenient, albeit not the simplest[18] way to set up the exchange problem theoretically is to treat it as a nonmutual exchange between four explicit three-spin configurations. The structure of the required matrices in composite spin Liouville space[20,23] is indicated schematically in Figure 3, where each box symbolizes a submatrix of order 3 or 9. A slightly modified version[24] of the iterative computer program DNMR5[21] was used for the calculations. This program, whose algorithm is constructed in such a way as to render divergence logically impossible, operates directly on the experimental spectra as produced by the NMR spectrometer, typically represented as 4K or 8K raw data points depending on resolution requirements, and automatically produces the optimum values for all those parameters which are specified as adjustable on input. The two parameters of greatest interest in the present context are the first-order rate constants k_5 and k_6 (Figure 3), but there is an additional complication in that the relative shift assignments are not known. To solve both problems simultaneously by the standard technique of spectral synthesis would be difficult if not impossible in view of the subtlety of the differences. Apart from eliminating the tedium of variations by hand, it is in the present context that automated methods come into their own, as will now be demonstrated in some detail.

The arsenic compound **5** will be considered first. In this case the XY labels of Figure 3 refer to the protons of the difluoromethyl substituents and the static parameters are those in rows 2 of Tables I and II, suitably extrapolated (see Experimental Section) to the appropriate temperature. Iterative band shape calculations were performed for both alternative shift assignments and the numerical rate results for four intermediate temperatures, bracketing the range in which the spectra are most sensitive to mechanism and assignment, are collected in Table V. For assignment 2 the rate

(16) "That process [*said Holmes*] starts upon the supposition that when you have eliminated all which is impossible, then whatever remains, however improbable, must be the truth." Doyle, Sir Arthur Conan "The Case-Book of Sherlock Holmes"; Penguin Books: Harmondsworth, 1973; p 57.

(17) This applies to the distinction between M_1 and M_2 as well, although in this case the difference is very subtle indeed and would in practice again require a study in liquid crystal solution.

(18) By exploiting the additional invariance properties[19] of the theory[20] resulting from the fact that the exchange as formulated really involves mutual as well as nonmutual processes and that the couplings to the third spin are strictly of first order, a further factorization of the equations beyond that routinely possible in the published DNMR5 computer program[21] would be feasible, but would require a more extensive redesign of the program. In view of the high efficiency of the algorithms developed by us[3,22] there was insufficient incentive for this investment of human effort and all calculations were therefore performed in a brute-force fashion, requiring the diagonalization of a complex nonhermitian matrix of order 36 for each function evaluation in the course of the iterations.

(19) Kleier, D. A.; Binsch, G. *J. Magn. Reson.* **1970**, *3*, 146–160.

(20) Binsch, G. *J. Am. Chem. Soc.* **1969**, *91*, 1304–1309.

(21) Stephenson, D. S.; Binsch, G. *QCPE* **1978**, *10*, 365.

(22) Stephenson, D. S.; Binsch, G. *J. Magn. Reson.* **1978**, *30*, 625–626.

(23) Binsch, G. In "Dynamic Nuclear Magnetic Resonance Spectroscopy", Jackman, L. M., Cotton, F. A., Eds.; Academic Press: New York, 1975; pp 45–81.

(24) This version accepts seven independent rate parameters and automatically places them in their correct positions in the matrices as dictated by the mechanisms. All k values can be specified as variable, thus enabling the program to handle arbitrary linear combinations of all seven mechanisms.

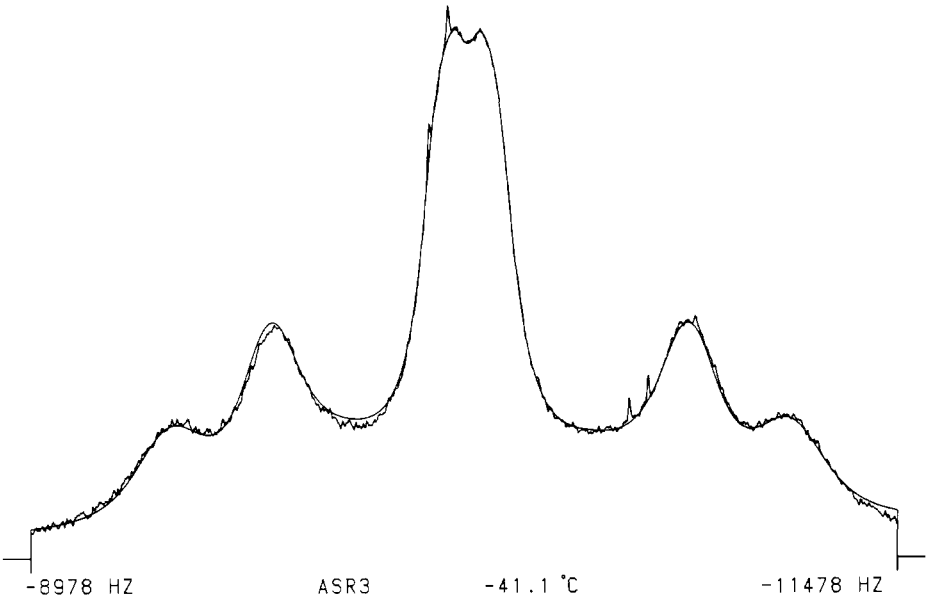

Figure 4. Observed and superposed computed 94.08 MHz ^{19}F DNMR spectra of **5** in acetone-d_6 at −41.1 °C.

parameter k_6 converged to zero within one standard deviation. Although the errors in the rate constants for assignment 1 are about 2 to 3 times as large as those for assignment 2, the overall fit of the computed on the experimental band shapes remains quite good for assignment 1 as well and would in fact meet the most rigorous standards applied in the synthetic approach of the past, but the rate parameters now exhibit an erratic pattern; in particular, k_5 is found to decrease with increasing temperature in the interval from −38.6 to −31.4 °C. This physically nonsensical result can only mean that assignment 1 is incorrect, which in turn implies that M_5 must be the correct mechanism. Assignment 2 corresponds to that used in the labeling of Tables I, II, and IV.

A typical example of an experimental spectrum and of a theoretical band shape, calculated for assignment 2 and superposed by computer, is shown in Figure 4. For the most intense peak in the center the two traces are virtually indistinguishable to the unaided eye on the scale they are reproduced in this paper. In spite of the four spikes visible in the experimental spectrum, which arise from the decomposition product already alluded to, the overall agreement factor[12] is 0.0006. Throughout the entire temperature range of the dynamic study the R factor for assignment 2 never exceeded 0.3%, and that observation establishes another point. Although the fast-exchange limit spectra strongly suggest that either M_5 or M_6 or both are involved, they do not logically exclude the possibility of a contribution from the other mechanisms or even of a suitable mixture of mechanisms excluding M_5 and/or M_6. The superb agreement between experiment and theory for M_5 alone, however, leaves no room for a measurable contribution from any mechanism other than M_5.

Owing to the presence of long-range couplings (Table III), compounds **4**, **6**, and **7** required a slightly different approach. For **4** and **6** ^{31}P was chosen as the hetero nucleus X = Y in the matrix of Figure 3 and the computed band shapes were displaced by the average value of the four $^2J_{HF}$ couplings and superposed. Since the individual J_{HF} parameters of Table II differ from this average by less than 1 Hz, whereas the dynamic spectra cover a range of about 2.5 kHz, the error introduced by this approximation is totally negligible for the dynamic results. An additional approximation was necessary for **7**. Although the DAVINS program[12] used in the static analysis can handle any spin with quantum numbers up to $^9/_2$, DNMR5[21] was only designed for spins $^1/_2$. The presence of ^{75}As therefore had to be simulated by an X = Y pseudospin $^1/_2$ having J_{AsF} values twice those actually measured and by a slightly larger line width parameter for the fine-structure components, which was adjusted by a separate least-squares calculation. Since the actual F–As splittings are quite small (Table III) and are washed out at the very onset of exchange broadening, before accurate rate and mechanism studies become possible, this approximation also proved to be perfectly acceptable in practice.

The static and dynamic spectra of **5** are accidentally almost symmetric with respect to the midpoint (Figures 2 and 4) and this feature militates against the development of major differential effects. A rigorous answer to the mechanism and assignment problem could only be obtained because of the excellent S/N ratio attainable in this case. The spectra of **6** and **7** are less critical in this regard, partly because of the presence of additional fine structure but mainly owing to the asymmetry induced by the pattern of chemical shifts (Table I). For **6** and **7** we shall therefore present the evidence in pictorial rather than tabular form.

A small subset of spectra for **6** at four temperatures is shown in Figure 5 in compressed format, with the assignment implied in Tables I–IV on the left and with the reversed assignment on the right. Up to about 70 °C there is no noticeable difference, the computed curves for both assignments matching the spectrum at 66.2 °C about equally well. This is indeed precisely what one expects theoretically. It has been known for a long time[1] that the incipient line broadening caused by exchange is independent of chemical shift differences. It is only after the lines begin to show significant overlap that the spectra become sensitive to assignments and mechanisms, as visible at 79.7 and 95.9 °C. On the left the fit remains perfect and k_6 converged to zero, whereas on the right the iterative algorithm can only produce the best compromise in trying to match the experimental spectra with curves computed on the basis of an incorrect theoretical model. Toward the fast-exchange limit the differences diminish again and eventually vanish, as seen from the traces applicable to 117.5 °C. The spectra of **7** are even more favorable in regard to asymmetry (Figure 6). Here we also show a spectrum at the onset of exchange broadening (14.8 °C), just after the fine structure caused by ^{75}As has disappeared, in order to demonstrate the validity of the approximation of treating the arsenic nucleus as a pseudospin $^1/_2$. The remaining three spectra of Figure 6 again establish the assignment of Table I and the exclusive operation of mechanism M_5.

A corresponding study of **4** remained inconclusive, owing to experimental difficulties. The relatively fast decomposition in solution already mentioned forced us to record the spectra rather rapidly, with the attendant deterioration in quality, which proved to be insufficient for a rigorous distinction. Here we can only state that the results are fully consistent with mechanism M_5, but we cannot claim to have proved it beyond the shadow of a doubt.

Pulse Experiments. Whereas it is clear that a rigorous answer to a mechanistic problem, in which several processes may be involved simultaneously, can only come from a quantitative measurement, it might appear intellectually disconcerting that a distinction between two mutually exclusive assignments should also have to rest on the outcome of a black-box iterative calcu-

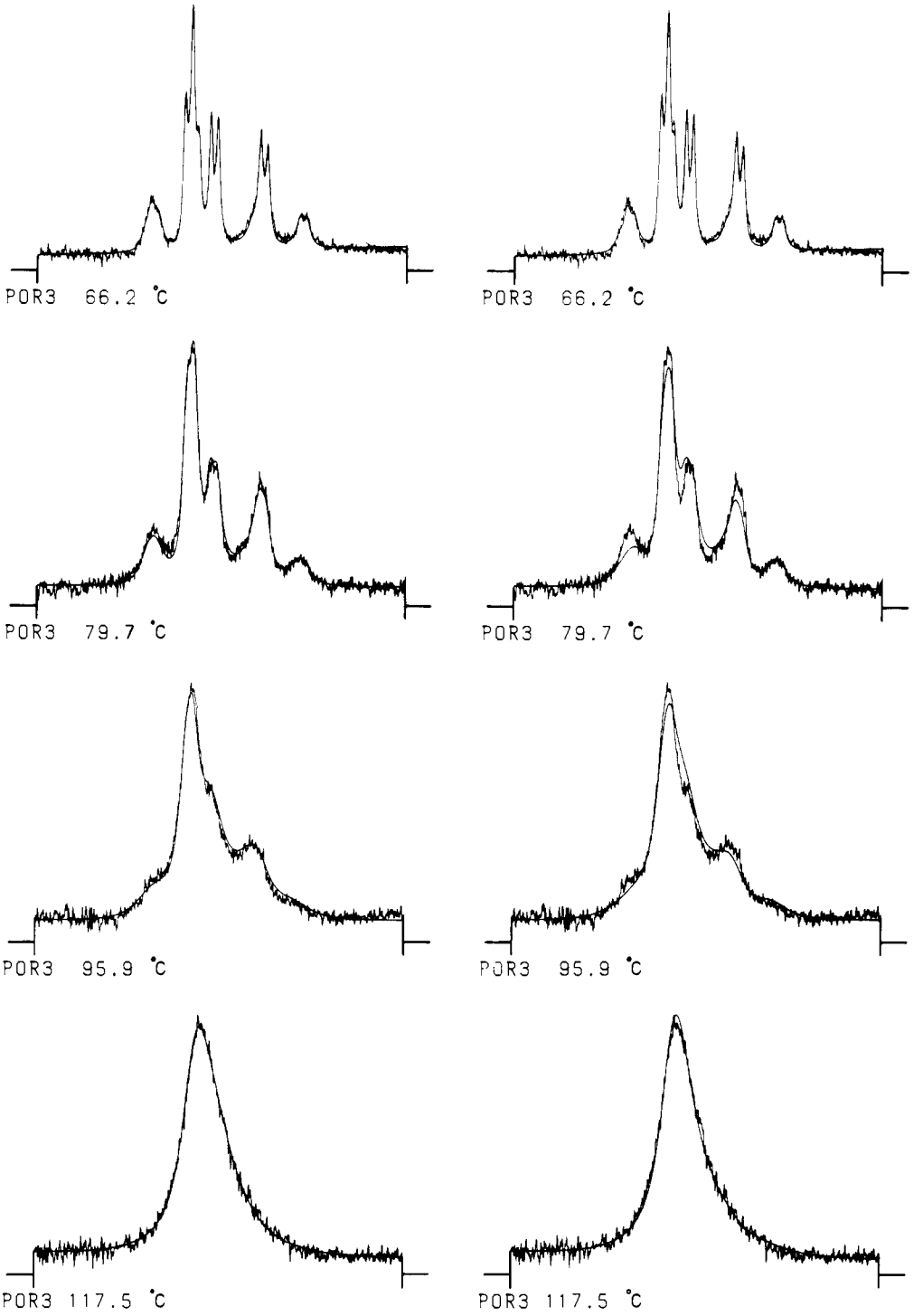

Figure 5. Observed and superposed computed 94.08 MHz ^{19}F DNMR spectra of **6** in acetone-d_6. The theoretical band shapes of the set on the left were computed with the chemical shift assignment of Table I and those of the set on the right with an assignment in which the labels C and D are interchanged.

lation. The classic work of Forsén and Hoffman on saturation transfer[25] indeed suggests the possibility of obtaining a more direct answer to the latter question. With the availability of modern pulse techniques it is preferable to invert certain lines rather than only saturate them, since this version yields twice the sensitivity of the original experiment.

The Forsén–Hoffman theory[25] is, however, only applicable to singlets or to first-order coupled systems. A qualitative interpretation of the results is particularly straightforward in such cases, since each line in the spectrum can be uniquely associated with a single nucleus in the molecule. This does not apply to the spin systems encountered in the present work, where quantum-mechanical mixing of the primitive spin product functions obscures the relationship. Nevertheless, since we were only interested in obtaining a qualitative answer, it was conceivable that a first-order approximation might prove adequate. Preliminary pulse experiments were therefore performed on **5** at −77 °C, but it was found that the observed effects were exceedingly subtle and could not be understood on a first-order basis. It became clear that if one persisted in this endeavor, an explicit quantum-mechanical treatment was unavoidable.

(25) Forsén, S.; Hoffman, R. A. *Acta Chem. Scand.* **1963**, *17*, 1787–1788; *J. Chem. Phys.* **1963**, *39*, 2892–2901; **1964**, *40*, 1189–1196. Hoffman, R. A.; Forsén, S. *Ibid.* **1966**, *45*, 2049–2060.

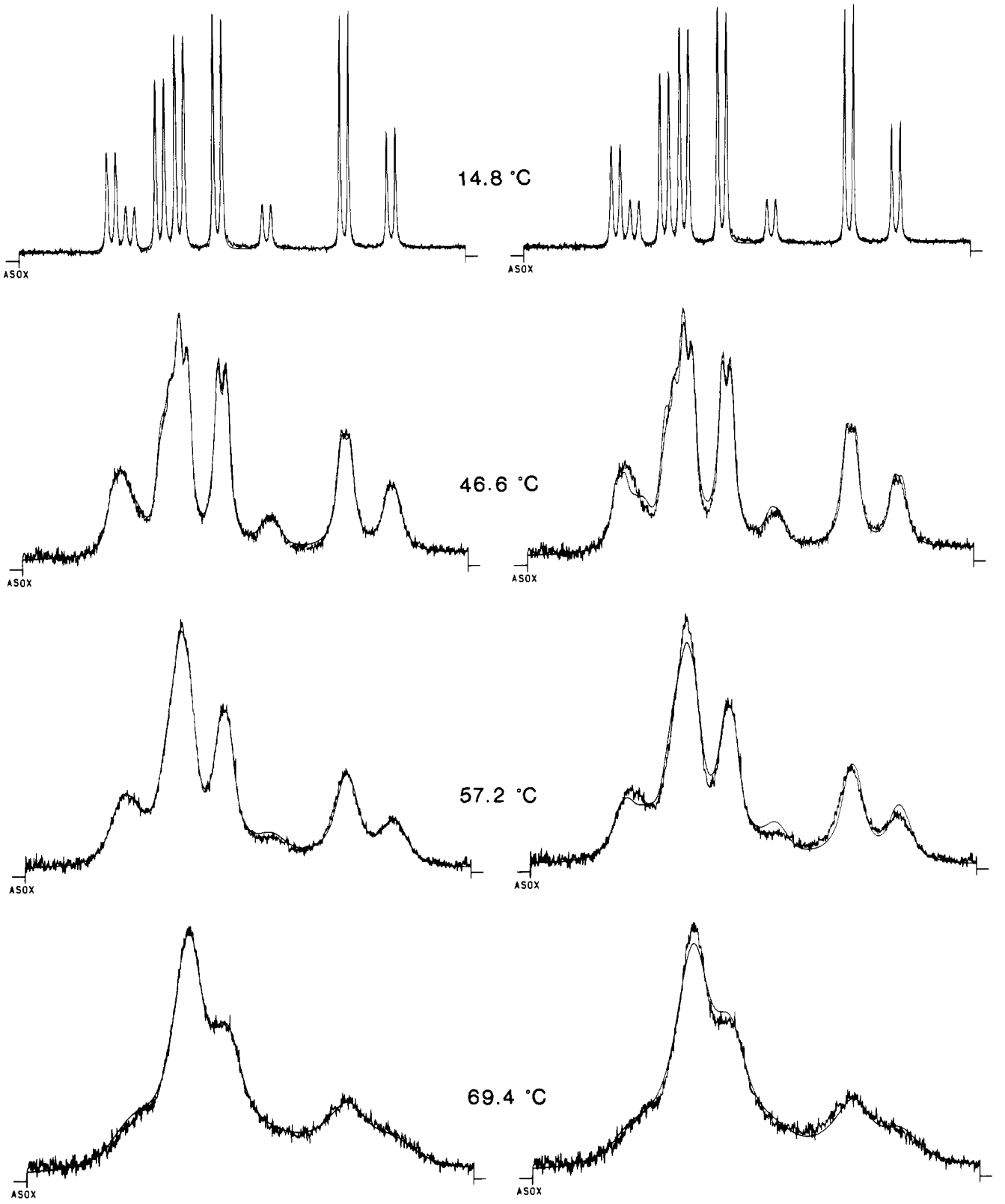

Figure 6. Observed and superposed computed 94.08 MHz ^{19}F DNMR spectra of **7** in acetone-d_6. The theoretical band shapes of the set on the left were computed with the chemical shift assignment of Table I and those of the set on the right with an assignment in which the labels C and D are interchanged.

The skeleton of a density matrix theory of selective population inversion for chemical exchange (SPICE) is outlined in the Appendix. A computer program was written which allows the calculation of synthetic spectra as a function of evolution time and initial conditions. The value of the "global" longitudinal relaxation time T_1 needed in these calculations was measured by a standard nonselective inversion–recovery pulse experiment and found to be 110 ms at −77 °C. The rate constant k_5 at that temperature was back-calculated from the activation parameters to be presented in the next subsection. The program was then used to determine the optimum initial settings and the range of evolution times for which one expects the most pronounced differences between the two assignments. It was discovered that this was the case for a *simultaneous* inversion of lines 1 and 3, counted from the left, and for evolution times between 15 and 80 ms. Some calculated spectra for both assignments are shown in Figure 7.

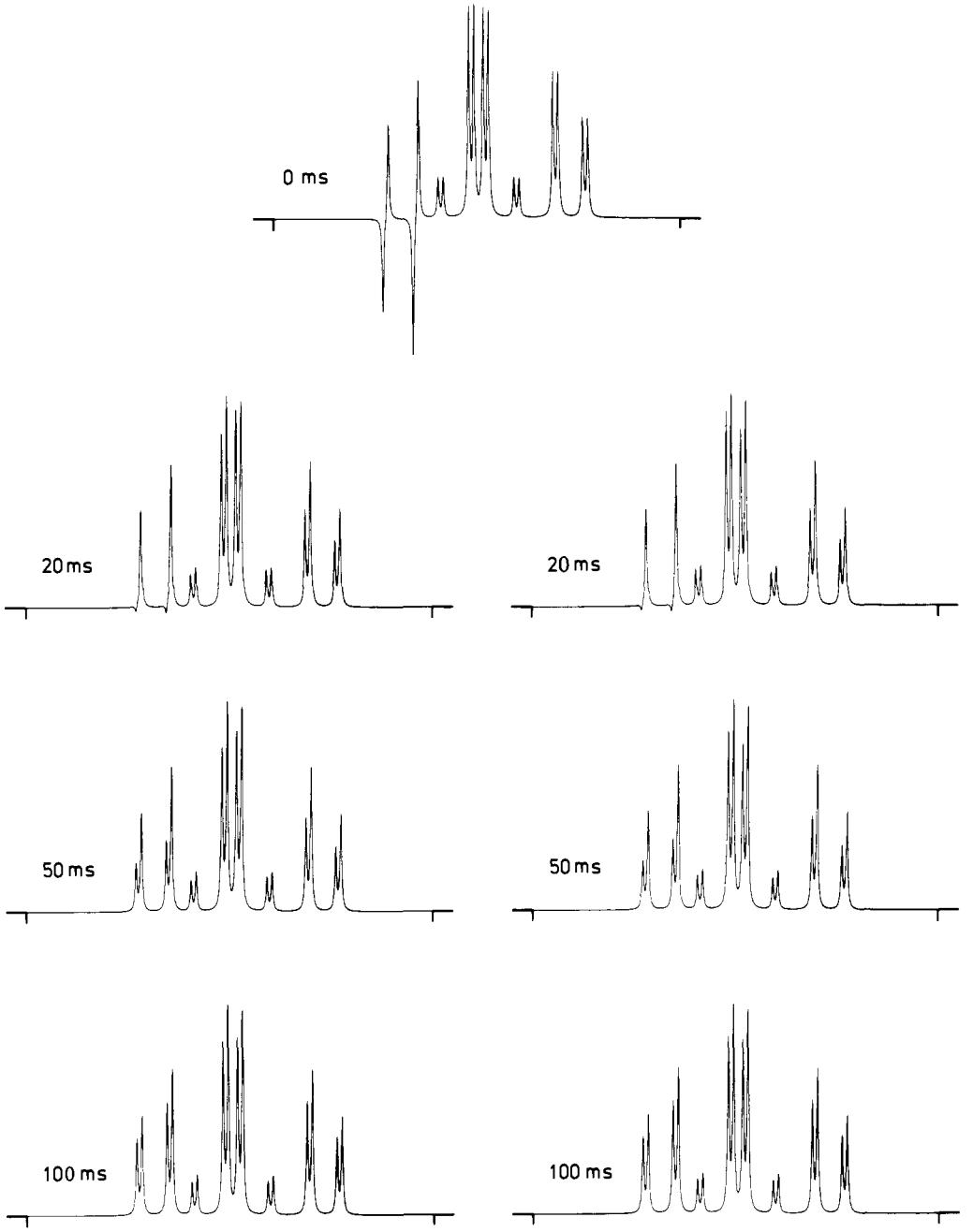

Figure 7. Computed time-dependent ^{19}F NMR spectra of **5** as a function of evolution time τ. The left set is based on the assignment of Table I and the right set on an assignment in which the labels C and D are interchanged.

Knowing exactly what to look for experimentally, a suitable DANTE pulse sequence[26] was programmed (see Experimental Section) for selectively inverting lines 1 and 3. Two experimental spectra are shown in Figure 8. As can be seen, the agreement is not quantitative and is indeed not expected to be so in view of the simplifying approximations made in the theoretical treatment (see Appendix), but the experimental spectra are in qualitative accord with the left set of Figure 7 and in qualitative discord with the right. The left set corresponds to the assignment also found in the band shape studies.

Activation Parameters. The temperature ranges over which the iterative band shape calculations produced rate errors of <10% and the activation parameters obtained by a properly[1] weighted least-squares fit of the k_5 values to the Eyring equation are given in Table VI. The activation enthalpies follow the pattern expected from the difference in the C–P and C–As bond lengths and from the smaller "size" of a free electron pair as compared to an oxygen atom. The differences between the entropies of activation, on the other hand, are not statistically significant and it is therefore only justified to consider their weighted average of −7.28 cal mol^{-1} K^{-1} as arising from a fundamental property shared by all four compounds. The sign and magnitude of this number can be rationalized on the basis of the following arguments.

Table VI. Activation Parameters and Their Standard Deviations

compd	temp range, °C from	to	$\Delta H^{\ddagger}$, kcal mol^{-1}	$\Delta S^{\ddagger}$, cal mol^{-1} K^{-1}
4	−21.9	67.3	10.37 (0.28)	−8.19 (0.96)
5	−56.6	23.5	8.69 (0.12)	−7.80 (0.46)
6	60.1	107.4	14.02 (0.08)	−7.24 (0.23)
7	34.3	106.4	13.01 (0.12)	−6.95 (0.35)

First there are the trivial effects arising from the chriality of the ground state and from its rotational symmetry number (or, equivalently, from the degeneracy of M_5), yielding terms of $-R$ ln 2 and $+R$ ln 3, respectively, for a combined contribution of

(26) Morris, G. A.; Freeman, R. *J. Magn. Reson.* **1978**, *29*, 433–462.

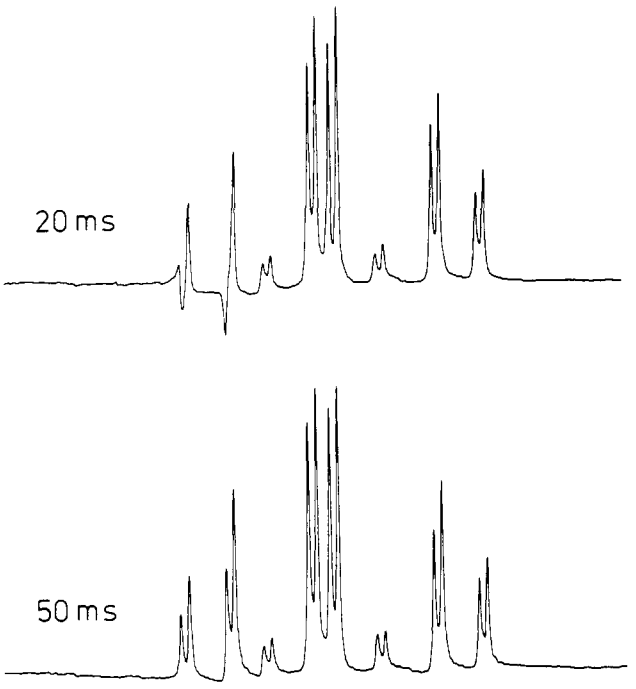

Figure 8. Observed time-dependent 94.08 MHz ^{19}F NMR spectra of **5** in acetone-d_6 at −77 °C as a function of evolution time τ.

+0.81 cal mol^{-1} K^{-1}. This leaves a value of −8.09 to be explained by other causes. The translational term is of course zero and the contribution from the difference in the moments of inertia of the ground and transition states is expected to be altogether negligible, as was indeed verified by explicit calculation. Internal rotation of the difluoromethyl groups is more difficult to judge, even in regard to sign, but order-of-magnitude calculations, using the Pitzer–Gwinn tables[27] and making rather extreme assumptions in regard to the barrier differences in the ground and transition states, render it unlikely that this effect can account for substantially more than one entropy unit. There only remains vibration. Again, because one is looking at differences, most modes can be safely neglected. But there is one exception, namely that normal vibration in the ground state which becomes the reaction coordinate. At the transition state this mode has be definition a negative force constant k and hence an imaginary frequency ω; in other words, it is completely lost and must therefore contribute a large negative entropy term. In the present instance the relevant mode is a torsional oscillation, whose frequencies are typically found[28] in the far infrared. Because of the large reduced mass μ of three ortho-disubstituted phenyl rings, which occurs in the denominator of the frequency formula $\omega = (k/\mu)^{1/2}$, the frequency of this mode should be pushed down to the very far infrared or perhaps even into the microwave region. Indeed, if one uses the measured activation entropy in the Einstein formula[29]

$$S_{vib} = R[x/\{\exp(x) - 1\} - \ln\{1 - \exp(-x)\}]$$

where

$$x = hc\omega/k_BT$$

and where the symbols have their standard meanings, one calculates a value of ω of about 10 cm^{-1}.

The foregoing discussion can at best be no more than what it claims to be, namely a crude attempt at rationalization, but the result is in line with previous experience in this laboratory[30] indicating that entropies of activation of conformational processes in solution can be understood, not only qualitatively but semiquantitatively.

Experimental Section

NMR Measurements. A Varian XL-100/VDM 620 L-100 spectrometer–computer system equipped with 32K of central memory, a disk unit, and a magnetic tape drive was used. The sample solutions consisted of 5–10% of the compounds in acetone-d_6 and were degassed by three freeze–thaw cycles. They were contained in 5 mm o.d. precision NMR tubes, which were sealed under reduced pressure. Chemical shifts are referred to internal Me_4Si for ^1H, to external 15:85 $CFCl_3$–acetone-d_6 for ^{19}F, and to external 85% H_3PO_4 for ^{31}P. Temperatures were measured by the substitution method,[1] using a Fluke Model 2100A-03 digital thermometer and a calibrated copper–constantan thermocouple immersed in an open NMR tube containing toluene and mounted such that its measuring junction was situated 9 mm from the bottom. All spectra were recorded in FT mode. Typically, 16–128 transients were accumulated for the static and 256–2048 for the dynamic ^{19}F spectra. The length of the data vector was 32K for the static and 8K and 16K for the dynamic measurements, depending on the degree of fine structure present in the spectra. The spectral points obtained after Fourier transformation and phase adjustment were initially stored on the disk. At the end of a work session on the spectrometer the spectra were copied to a magnetic tape, separated by end-of-file marks. This tape was then physically carried to the computing center for further processing.

The standard nonselective inversion–recovery pulse technique was used in the determination of the global T_1 for **5** at −77 °C. Employing commercial software, a separate T_1 was calculated for each of the 12 major peaks. The cited value of 110 ms represents the average.

Computations. All static and steady-state dynamic ^{19}F NMR spectra were subjected to automated analysis[3,12] on a CDC CYBER 175 computer, using slightly modified versions of published computer programs.[12,21] The chemical shifts and coupling constants and an effective transverse relaxation time T_2^{eff} were in each case calculated iteratively at five temperatures below the onset of exchange broadening, covering the ranges from −80.4 to −51.6 °C for **4**, from −91.7 to −75.3 °C for **5**, from −21.9 to 15.5 °C for **6**, and from −23.3 to 14.8 °C for **7**. The coupling constants and T_2^{eff} showed no statistically significant variation with temperature; these parameters could thus be treated as constants in the dynamic calculations. Most chemical shifts, on the other hand, were found to exhibit a systematic temperature dependence. They were therefore specified as adjustable also in the iterative DNMR5[21] calculations, together with the rate and base line parameters,[3] up to the point where there was still sufficient fine structure. Beyond that point extrapolated chemical shifts had to be used, calculated from a least-squares fit of the values at lower temperatures to a linear function of T.

The time-dependent synthetic spectra of Figure 7 were calculated using a computer program based on the theory presented in the Appendix. That theory is applicable to the downfield subspectrum, whereas the upfield subspectrum, displaced by the average value of J_{HF} from the former, remains unaffected. The final curves were obtained by superposition. The activation parameters were calculated using the program ACTPAR,[1] rewritten in BASIC for a Tektronix Model 4051 S computer. The standard deviations of the rate constants required on input were those automatically produced by DNMR5. The standard deviations of the temperatures were estimated from the differences in the temperature readings before and after recording a spectrum, as determined by the substitution technique.

DANTE Pulse Sequence.[26] As a preparation, general assembler-coded software was written for selectively inverting up to five individual lines (or regions) of a spectrum. In merging the separate pulse trains, due account must be taken of the software overhead in the execution loops, which was 30 μs on our instrument. Two pulses whose calculated separation was less than this amount therefore had to be replaced by a single average pulse of twice the width. The small amount of jitter inevitably introduced thereby was experimentally found not to be serious, but it required a slight trial-and-error readjustment of the theoretically calculated repetition rates and pulse numbers for optimum performance.

The carrier frequency was offset by 2931.7 Hz toward the right from the leftmost peak in the spectrum (No. 1), yielding a pulse separation of 341.1 μs for the first train and a corresponding number of 379.4 μs for the second (for line No. 3, counted from the left). The standard power level of the transmitter was too high for the desired selectivity, whose lower limit was predetermined by the requirement of not hitting the next fine structure line separated by J_{HF}, but could be reduced to an acceptable level, corresponding to 35 μs for a nonselective 90° pulse, simply by detuning the transmitter network. The number of pulses in each train is predicted to be inversely proportional to the transition matrix

(27) Pitzer, K. S.; Gwinn, W. D. *J. Chem. Phys.* **1942**, *10*, 428–440.
(28) Allen, G.; Fewster, S. In "Internal Rotation in Molecules", Orville-Thomas, W. J., Ed.; Wiley: New York, 1974; pp 255–283.
(29) Stull, D. R.; Westrum, E. F.; Sinke, G. C. "The Chemical Thermodynamics of Organic Compounds"; Wiley: New York, 1969; p 101.
(30) (a) Höfner, D.; Tamir, I.; Binsch, G. *Org. Magn. Reson.* **1978**, *11*, 172–178. (b) Höfner, D.; Lesko, S. A.; Binsch, G. *Ibid.* **1978**, *11*, 179–196.

elements, for which one calculates a ratio of 0.84. The numbers actually used in the experiment were 68 1-μs pulses for line No. 1 and 60 1-μs pulses for line No. 3, for a combined pulse train of 23 ms total duration. An 18° nonselective observing pulse (7 μs) was used, followed by an acquisition time of 0.5 s and a pulse delay of 1 s, and the total sequence was repeated 32 times.

2-Bromoisophthalaldehyde. A solution of 165 g (1.6 mol) of CrO_3 in 500 mL of acetic anhydride, prepared by slowly adding the former in small portions to the latter under cooling, was added, with stirring and cooling in an ice bath, to a cold mixture of 50 g (0.27 mol) of 2,6-dimethylbromobenzene, 500 mL of acetic anhydride, and 135 mL of concentrated H_2SO_4 over a period of 3 h. After being stirred for another 2 h at 15 °C the mixture was poured onto 4 kg of ice and left standing for 12 h. The crude crystalline material (ca. 71 g) obtained on filtration was subjected to acid hydrolysis by boiling it in a mixture of 400 mL of dioxane and 100 mL of concentrated aqueous HCl for 4 h. Most of the solvent was removed on the rotary evaporator and 300 mL of water were added. The precipitate was collected on a filter, thoroughly washed with water, and dried in a vacuum desiccator over $CaCl_2$. The crude product was taken up in CH_2Cl_2 and the solution passed through a short column packed with alumina. The solvent was evaporated and the residue was recrystallized from EtOH to yield 35.7 g (0.17 mol, 62%) of pale yellow needles: mp 137.5–138.5 °C; IR (KBr) 1700 (s), 1676 (s) cm^{-1}; ^1H NMR ($CDCl_3$) δ 10.43 (s, 2, CHO), 7.38–8.15 (AB_2 pattern, 3, ArH); mass spectrum (70 eV) *m/e* 214 (97%, M^+), 213 (73%, $M^+ - H$), 212 (100%, M^+), 211 (71%, $M^+ - H$), 186 (15%, $M^+ - CO$), 185 (9%, $M^+ - H, CO$), 184 (15%, $M^+ - H, HCO$), 104 (18%, $M^+ - Br, HCO$), 75 (40%, $M^+ - 2\,HCO, Br$), 76 (57%, $M^+ - CO, HCO, Br$), 29 (10%, CHO^+). Anal. ($C_8H_5BrO_2$) C, H.

2,6-Bis(difluoromethyl)bromobenzene. The reaction vessel was a steel autoclave of 300 mL contents horizontally mounted on the board of a motor-driven shaker and encased in an electric heating mantle whose temperature could be electronically controlled to within ±2 °C. A mixture of 10.0 g (46.9 mmol) of 2-bromoisophthalaldehyde, 50 mL of CH_2Cl_2, and 23 drops of water was placed in the opened vessel. The cap with the pressure gauge was screwed on, the autoclave attached to a vacuum line, and the vessel cooled to −78 °C and evacuated. A trap also attached to the vacuum line contained 22.0 g (203 mmol) of liquefied SF_4, which was allowed to condense slowly into the cooled autoclave. The valve was closed and the vessel was allowed to return to room temperature and then shaken at 83–85 °C for 9 h. After venting the excess of SF_4 the mixtures was taken up in CH_2Cl_2, washed with 5% aqueous $NaHCO_3$ solution and water, and dried (Na_2SO_4). The crude yield was essentially quantitative, but VPC showed four volatile impurities totaling about 15%. Samples from several runs were combined and subjected to careful fractional vacuum distillation on a high-efficiency concentric tube (Fischer) column to yield about 60% of pure colorless liquid: bp 84–85 °C (1 mmHg); ^1H NMR ($CDCl_3$) δ 7.31–7.80 (AB_2 pattern, 3, ArH), 6.88 (t, 2, $^2J_{HF}$ = 54.5 Hz, CHF_2); ^{19}F NMR (acetone-d_6) δ −115.35 (d, 4, $^2J_{HF}$ = 54.5 Hz, CHF_2); mass spectrum (70 eV) *m/e* 258 (98%, M^+), 256 (100%, M^+), 177 (18%, $M^+ - Br$), 176 (36%, $M^+ - HBr$), 239 (11%, $M^+ - F$), 237 (11%, $M^+ - F$), 238 (20%, $M^+ - HF$), 236 (19%, $M^+ - HF$), 126 (13%, $M^+ - CHF_2, Br$), 107 (12%, $M^+ - CHF_2, F, Br$), 75 (8%, $M^+ - 2CHF_2, Br$), 51 (8%, CHF_2^+). Anal. ($C_8H_5BrF_4$) C, H.

Tris[2,6-bis(difluoromethyl)phenyl]phosphine (4). A solution of 2.98 g (11.6 mmol) of 2,6-bis(difluoromethyl)bromobenzene in 4 mL of anhydrous Et_2O was treated with an equimolar amount of *n*-butyllithium (as a ca. 1.5 M solution in *n*-hexane) at −40 °C under N_2 and stirred for 2 h at −30 °C. A solution of 397 mg (2.89 mmol) of PCl_3 in 2 mL of anhydrous Et_2O was then added over a period of 15 min at −30 °C. The mixture was stirred for 10 h at 25 °C and for 8 h at reflux temperature, then hydrolyzed with saturated aqueous NH_4Cl solution and diluted with CH_2Cl_2. The organic layer was separated and dried (Na_2SO_4). Removal of the solvent left 2.4 g of a red oil, whose VPC showed the presence of at least ten components in comparable amounts. Repeated trituration with pentane and EtOH caused partial crystallization. Two recrystallizations from EtOH yielded 300 mg of brown crystals of melting range 175–195 °C. Column chromatography on alumina (activity IV, 150 g, CCl_4) produced enriched material in the early fractions, which on further recrystallizations from EtOH left 20 mg (2%) of pure compound as colorless needles: mp 233–234 °C; ^1H NMR at −71 °C (acetone-d_6) δ 8.0 (m, 9, ArH), 7.79 (dt, 3, $^4J_{HP}$ = 6.5 Hz, $^2J_{HF}$ = 53.6 Hz, CHF_2), 6.35 (t, 3, $^2J_{HF}$ = 53.8 Hz, CHF_2); ^1H NMR at 65 °C (acetone-d_6) δ 7.93–8.05 (AB_2 pattern, 9, ArH), 6.95 (dt, 6, $^4J_{HP}$ = 3.2 Hz, $^2J_{HF}$ = 54.0 Hz, CHF_2); ^{31}P NMR {^1H} at 28 °C (acetone-d_6) δ −42.87 (m, 1, $^4J_{FP}$ = 11.8 Hz); mass spectrum (70 eV) *m/e* 562 (83%, M^+), 543 (7%, $M^+ - F$), 511 (100%, $M^+ - CHF_2$), 334 (5%, $M^+ - C_8H_5F_4, CHF_2$), 177 (2%, $C_8H_5F_4^+$). Anal. ($C_{24}H_{15}F_{12}P$) C, H.

Tris[2,6-bis(difluoromethyl)phenyl]arsine (5). A procedure analogous to that used in the preparation of **4**, using 2.95 g (11.5 mmol) of 2,6-bis(difluoromethyl)bromobenzene and 520 mg (2.87 mmol) of $AsCl_3$, resulted in 2.64 g of an oil which partially crystallized on prolonged standing. Six recrystallizations from EtOH yielded 370 mg (22%) of colorless needles: mp 189.5–190 °C; ^1H NMR at −79.4 °C (acetone-d_6) δ 8.0 (m, 9, ArH), 7.65 (t, 3, $^2J_{HF}$ = 53.8 Hz, CHF_2), 6.41 (t, 3, $^2J_{HF}$ = 53.8 Hz, CHF_2); ^1H NMR at 30 °C (acetone-d_6) δ 7.88–8.08 (AB_2 pattern, 9, ArH), 6.93 (t, 6, $^2J_{HF}$ = 54.5 Hz, CHF_2); mass spectrum (70 eV) *m/e* 606 (73%, M^+), 587 (1%, $M^+ - F$), 316 (18%, $C_{16}H_{10}F_6^+$), 296 (34%, 316 − HF), 265 (100%, 316 − CHF_2), 246 (36%, 316 − F, CHF_2), 177 (6%, $C_8H_5F_4^+$), 51 (4%, CHF_2^+). Anal. ($C_{24}H_{15}AsF_{12}$) C, H.

Tris[2,6-bis(difluoromethyl)phenyl]phosphine Oxide (6). Oxidation of 20 mg of **4** in 2.5 mL of acetone with 0.2 mL of 30% aqueous H_2O_2 for 8 h at 45 °C produced pure **6** in quantitative yield. The product was recrystallized from EtOH: mp 231–231.5 °C; ^1H NMR at 30 °C (acetone-d_6) δ 7.98–8.32 (m, 9, ArH), 7.62 (t, 3, $^2J_{HF}$ = 55.0 Hz, CHF_2), 6.40 (t, 3, $^2J_{HF}$ = 55.0 Hz, CHF_2); ^{31}P NMR at 28 °C (acetone-d_6) δ −28.29 (s, broad); mass spectrum (70 eV) *m/e* 578 (0.1%, M^+), 559 (8%, $M^+ - F$), 543 (1%, $M^+ - O, F$), 507 (100%, $M^+ - CHF_2, HF$), 178 (84%, $C_8H_6F_4^+$), 107 (17%, $C_7H_4F^+$), 47 (1%, PO^+). Anal. ($C_{24}H_{15}F_{12}OP$) C, H.

Tris[2,6-bis(difluoromethyl)phenyl]arsine Oxide (7). Oxidation of 80 mg (0.13 mmol) of **5** in 3 mL of acetone with 0.3 mL of 30% aqueous H_2O_2 for 16 h at 75 °C yielded 65 mg (80%) of **7** after recrystallization from EtOH: mp 240–242 °C; ^1H NMR at 30 °C (acetone-d_6) δ 7.93–8.27 (m, 9, ArH), 8.17 (t, 3, $^2J_{HF}$ = 53.8 Hz, CHF_2), 6.65 (t, 3, $^2J_{HF}$ = 54.3 Hz, CHF_2); mass spectrum (70 eV) *m/e* 622 (0.5%, M^+), 621 (5%, $M^+ - H$), 571 (38%, $M^+ - CHF_2$), 551 (6%, $M^+ - CHF_2, HF$), 425 (52%, $M^+ - C_8H_6F_4, HF$), 249 (100%, $M^+ - 2C_8H_6F_4, F$), 91 (1%, AsO^+). Anal. ($C_{24}H_{15}AsF_{12}O$) C, H.

Acknowledgment. Respects are paid to the participants in the Bat-Sheva Workshop on NMR (Kibbutz Nof Ginossar, Israel, 1979) to whom the problem was assigned as an exercise. This work was financially supported by the Fonds der Chemischen Industrie.

Appendix

Here we sketch the simple version of a density matrix theory of selective population inversion for chemical exchange (SPICE) which is adequate for the purpose at hand. In a more complete treatment, to be published elsewhere, explicit account needs to be taken of the dependence on the flip angle of the observing pulse and of the evolution of the system during the DANTE pulse sequence. Also, the way relaxation is handled in the present context is too simplistic to be satisfactory in general.

The starting point is the equation of motion of the density vector ρ in spin Liouville space[23] in the absence of radiation fields and after transient coherence phenomena have died out:

$$d\rho(t)/dt = \mathbf{X}\rho(t) + \mathbf{R}(\rho(t) - \rho_0(t)) \quad (1)$$

where **X** is the mutual exchange superoperator, **R** the relaxation superoperator, and $\rho_0(t)$ is the thermal equilibrium density vector. The latter is independent of time and is not affected by **X**:

$$\rho_0(t) = \rho_0(0) = \rho_0 \quad (2)$$

$$\mathbf{X}\rho_0 = 0 \quad (3)$$

Defining the deviation density vector η by

$$\eta(t) = \rho(t) - \rho_0 \quad (4)$$

and the hermitian superoperator **M** by

$$\mathbf{M} = \mathbf{X} + \mathbf{R} \quad (5)$$

eq 1 can be cast in the standard form of a matrix differential equation

$$d\eta(t)/dt = \mathbf{M}\eta(t) \quad (6)$$

whose solution is

$$\eta(t) = \exp(\mathbf{M}t)\eta(0) = \mathbf{V}\exp(\Lambda t)\mathbf{V}^\dagger\eta(0) \quad (7)$$

where

$$\mathbf{V}^\dagger\mathbf{M}\mathbf{V} = \Lambda = \mathrm{diag}[\lambda_1, \lambda_2, \ldots, \lambda_n] \quad (8)$$

and

$$\exp(\Lambda t) = \mathrm{diag}[\exp(\lambda_1 t), \exp(\lambda_2 t), \ldots, \exp(\lambda_n t)] \quad (9)$$

The preceding equations are invariant with respect to representation, but for an actual calculation one must of course decide on some specific representation. For the purpose of this Appendix the exchange is most conveniently formulated as occurring in an explicit four-spin system [ABCD] defining a 16-dimensional spin Hilbert space. The mechanism M_5 can then be characterized by the two schemes

$$\text{I:} \quad [ABCD] \rightleftharpoons [DCBA] \tag{10}$$

$$\text{II:} \quad [ABCD] \rightleftharpoons [BADC] \tag{11}$$

contributing with statistical factors of $^1/_3$ and $^2/_3$, respectively. The exchanges are most easily described by expressing the Hilbert space permutation operators P_I' and P_{II}' in a primitive spin product basis, hereafter distinguished by primes. We then get[23]

$$\mathbf{X}' = k_5(P_I' \otimes P_I'/3 + 2P_{II}' \otimes P_{II}'/3 - \mathbf{I}) \tag{12}$$

where the symbol $\otimes$ denotes a tensor product and $\mathbf{I}$ is the identity superoperator in spin Liouville space. For $\mathbf{R}'$ we take the representation-independent phenomenological form

$$\mathbf{R}' = -\mathbf{I}/T_1 = \mathbf{R} \tag{13}$$

which, naturally, can only be an acceptable approximation as long as relaxation does not dominate.

For specifying the deviation density vector $\eta(t)$ of eq 4 at time $t = 0$, right after an SPI by means of a DANTE pulse sequence, it is clearly more convenient to work in the eigenbasis of the static spin Hamiltonian $\mathcal{H}$. Referred to this eigenbasis, the equations need only be formulated in the 16-dimensional spin Liouville subspace spanned by the diagonal elements of the density matrix. It is then trivially easy to generate $\rho(0)$ by simple interchanges of the pertinent elements (corresponding to the inverted lines) in the thermal equilibrium spin density vector, which in the present instance assumes the form

$$\rho_0^{\dagger} = C(-2, -1, -1, -1, -1, 0, 0, 0, 0, 0, 0, 1, 1, 1, 1, 2) \tag{14}$$

apart from an irrelevant scaling factor C. So $\mathbf{X}'$ must be suitably transformed, which can be accomplished by a unitary supertransformation[19] in spin Liouville space:

$$\mathbf{X} = \mathbf{U}^{\dagger}\mathbf{X}'\mathbf{U} \tag{15}$$

where

$$\mathbf{U} = U \otimes U^* \tag{16}$$

and

$$U^{\dagger}HU = E_{\text{diag}} \tag{17}$$

Alternatively, the permutation operators may be transformed in spin Hilbert space:

$$P = U^{\dagger}P'U \tag{18}$$

and $\mathbf{X}$ calculated from the unprimed equation

$$\mathbf{X} = k_5(P_I \otimes P_I/3 + 2P_{II} \otimes P_{II}/3 - \mathbf{I}) \tag{19}$$

Registry No. 4, 79839-45-5; **5**, 79839-46-6; **6**, 79839-47-7; **7**, 79839-48-8; 2-bromoisophthalaldehyde, 79839-49-9; 2,6-dimethylbromobenzene, 576-22-7; 2,6-bis(difluoromethyl)bromobenzene, 79839-50-2.

Assignment of the Infrared Spectrum for the Ethyl Radical

J. Pacansky* and M. Dupuis

Contribution from IBM Research Laboratory, San Jose, California 95193.
Received March 18, 1981

Abstract: The infrared spectra of CH_3CH_2, CH_3CD_2, CD_3CH_2, and CD_3CD_2 have been observed in argon matrices by photolysis of the corresponding dipropionyl peroxides. The spectra of the isotopic species coupled with detailed ab initio calculations have provided the basis for an assignment. The analysis has revealed the spectral features that are clearly a manifestation of the unpaired electron.

Although the ESR spectrum of the ethyl radical has been reported by several groups,[1-3] only a few studies on the optical spectra of the ethyl radical exist. The electronic absorption spectrum, observed by Hunziker and Wendt,[4] and later by Parkes and Quinn,[5] revealed the presence of bands at 2060 and 2460 Å; presumably, the excitations could be described as a Rydberg and a valence transition, respectively. Owing to the diffuse nature of the bands, very little structural information could be gleaned from the electronic absorption studies.

The pertinent structural data that are needed to understand chemical reactivity of radicals pertains to the ground state. Toward this end, Pacansky, Bargon, and Gardini[6] reported the infrared spectrum of the ethyl radical. A preliminary analysis of this spectrum revealed that the structure of the ethyl radical could be described as consisting of a methyl and methylene group much like that in ethane and ethylene. Subsequently, Pacansky and Coufal[7] studied the deuterated species HCD_2CD_2 and concluded that the barrier for internal rotation about the C–C bond in the ethyl radical was very low or, most likely, nonexistent.

In this report, detailed experimental and theoretical studies are described on the ethyl radical in order to provide an assignment for the infrared absorptions. This assignment has provided very useful structural information for the ground state and has revealed the spectral features that are a manifestation of the unpaired electron.

Experimental Section

The various isotopically substituted dipropionyl peroxides were synthesized using the procedure developed by Johnson,[8] where KO_2 is used to convert an acid chloride to a diacyl peroxide. The propionyl chlorides were prepared using standard procedures[9] for converting acids to acid

(1) R. W. Fessenden and R. H. Schuler, *J. Chem. Phys.*, **39**, 2147 (1963).
(2) J. K. Kochi and P. J. Krusic, *J. Am. Chem. Soc.*, **91**, 3940 (1969).
(3) C. A. McDowell, P. Raghunathan, and K. Shimohoshi, *J. Chem. Phys.*, **58**, 114 (1973).
(4) H. E. Hunziker and R. Wendt, XIth International Symposium on Free Radicals, Berchtesgaden-Königssee, Sept 4-7, 1973.
(5) D. A. Parkes and C. P. Quinn, *J. Chem. Soc., Faraday Trans. 1*, **72**, 1952 (1976).
(6) J. Pacansky, J. Bargon, and G. P. Gardini, *J. Am. Chem. Soc.*, **98**, 2665 (1976).
(7) J. Pacansky and H. Coufal, *J. Chem. Phys.*, **72**, 5285 (1980).
(8) R. A. Johnson, *Tetrahedron Lett.*, 331 (1976).
(9) J. D. Roberts and M. C. Caserio, "Basic Principles of Organic Chemistry", W. A. Benjamin, New York, 1964.

0002-7863/82/1504-0415$01.25/0